Origin of the Barrier to Reactions of O_2 on Al(111): Charge Transfer not Spin Selection

Florian Libisch[1], Chen Huang[2], Peilin Liao[1], Michele Pavone[1,3], and Emily A. Carter[1*]
[1] *Departments of Mechanical and Aerospace Engineering and Chemistry, Program in Applied and Computational Mathematics, and Andlinger Center for Energy and the Environment, Princeton University Princeton, New Jersey 08544, USA*
[2] *Theoretical Division, Los Alamos National Laboratory, New Mexico 87544, USA*
[3] *Permanent address: Department of Chemistry, University of Napoli Federico II, Napoli 80120, Italy*
(Dated: August 13, 2012)

TECHNICAL DETAILS REGARDING THE EMBEDDING CALCULATION

In the following, we provide additional details on the density functional theory (DFT) and correlated wavefunction (CW) treatment of the O_2/Al(111) system. For the pure KS-DFT slab calculation, we use projector-augmented-wave (PAW) calculations as implemented in the VASP code [1] version 5.2 using default PAW potentials for Al and O. For all plane-wave (PW) DFT calculations, we use Fermi-Dirac smearing of 0.1 eV. We employ the Perdew-Burke-Ernzerhof (PBE) XC functional [2]. The Al (111) surface is modeled with a periodic 3×3 supercell containing seven Al layers separated by 20 Å of vacuum for a total of 63 atoms, a $6 \times 6 \times 1$ Monkhorst-Pack grid for k-point sampling (due to the large supercell, this is enough for a converged calculation), and a plane wave cutoff of 400 eV (without the PAW formalism, we would require a substantially higher cutoff). Al (111) is well-known to undergo negligible relaxation, making expensive surface reconstruction calculations unnecessary [3, 4]. To eliminate dipole interactions, a mirrored oxygen molecule is added on the other side of the slab. We perform a spin-polarized calculation to take into account the triplet ground state of O_2, although the entire system features a total magnetization $M_S = 0$ due to the presence of the two O_2 molecules.

For the embedded calculation, we consider an Al(111) periodic slab using a 5×5 supercell in the surface direction and four layers in the [111] direction (including 10 Å vacuum), with 100 atoms in the supercell. We used a larger unit cell than for the KS slab calculations to avoid artifacts in the embedding potential due to the periodic boundary conditions. An initial DFT treatment yields a reference ground state density ρ_{ref}. We use the abinit code [6, 7], and no PAW formalism, to be consistent with the subsequent calculation of the embedding potential. To confirm that the different choice of electron-ion potentials (VASP using PAW projectors vs. abinit using norm-conserving pseudopotentials) does not lead to a systematic error, we performed abinit calculations on the 3×3 slab (seven layers) plus oxygen system using the same non-local pseudopotentials as those used to determine the embedding potential (and an energy cutoff of 1000 eV). Apart from a constant global energy shift, we find (for the bridge site and parallel orientation) energy differences below 1 meV compared to the VASP energies as a function of $L_{\mathrm{O-O}}$ and $L_{\mathrm{Al-O_2}}$.

We then partition the bare slab (no O_2) into a small cluster containing 10 to 14 Al atoms with the remainder considered as the environment (we choose an even number of cluster atoms to avoid an open-shell cluster). We solve the cluster and environment independently, in the presence of a unique, global embedding potential V_{emb} [5]. We search for a V_{emb} that reproduces the reference density ρ_{ref} as the sum of the densities of cluster and environment. This algorithm has been implemented in a modified version of the abinit code [6, 7] (since it is more easy to modify than VASP) with PBE XC [2] and a Trouiller-Martins GGA [8] pseudopotential for Al, a plane-wave cutoff of 700 eV, and a $3 \times 3 \times 1$ Monkhorst-Pack grid for k-point sampling.

V_{emb} is then supplied to a modified MOLCAS code [9] for CW calculations on the embedded cluster. To obtain the CW-corrected final energy

$$E_{\mathrm{emb}} = E^{\mathrm{DFT}} + E^{\mathrm{CW}}_{\mathrm{emb}} - E^{\mathrm{DFT}}_{\mathrm{emb}}, \qquad (1)$$

we additionally perform embedded KS-DFT calculations using a modified GAMESS code [10, 11]. In both cases we use the same Stevens-Basch-Krauss-Jasien-Cundari (SBKJC) effective core potentials (ECPs) and polarizable basis sets (2s3p2d) for O and the closest Al atoms [12], and a smaller Los Alamos National Laboratory 2 Double-ζ (LANL2DZ) basis set (2s2p) and ECPs for the remaining Al atoms [13]. With MOLCAS, we perform CASSCF calculations choosing 16 electrons in 12 orbitals (denoted as 16/12), including the σ, σ^* and all π and π^* of O_2, as well as four HOMOs and two LUMOs from the metal cluster. We tested both smaller and larger CAS sizes, and found that the 16/12 choice gave a favorable combination of accuracy and efficiency. The CW energy is obtained using CASPT2 [13], i.e., second order multi-reference many-body perturbation theory, including an imaginary energy shift of 0.25 to prevent divergent denominators in the perturbative expansion [14].

Care must be taken to obtain a suitable initial guess for the CASSCF calculations. A bad guess will easily result in exceedingly slow convergence, no convergence,

or convergence to an unphysical solution (featuring, e.g., finite spin excitations on the metal cluster in the ground state). To solve this problem, we start with a minimal CAS, and then gradually add orbitals until the final CAS size is reached. We use a first qualitative guess based on atomic orbitals, to easily identify the two π^* orbitals that should become singly occupied at large $L_{\mathrm{Al-O_2}}$, in line with the triplet ground state of isolated O_2. Based on this starting guess, we perform an unrestricted open-shell Hartree-Fock calculation of the embedded system, for $L_{\mathrm{Al-O_2}} = 5$ Å, with a total spin $S = 1$ (i.e., a triplet). The resulting orbitals allow us to identify the remaining σ, σ^*, π and π^* orbitals of O_2 for a subsequent CASSCF calculation, with a CAS size of eight $2p$ electrons of the O_2 in six O_2 molecular orbitals. Having optimized the orbitals centered around O_2, we proceed with a RASSCF calculation using the previous six main CAS orbitals, as well as allowing single and double excitations from six occupied and four unoccupied orbitals of the metal cluster. The above involved procedure guarantees a physical spin configuration: namely, the Mulliken spin is completely localized at the O_2 molecule that features a triplet ground state at large $L_{\mathrm{Al-O_2}}$. The so-obtained molecular orbitals can now be used as input for a conventional CASSCF calculation. To effectively map out a large potential energy surface, we gradually (in steps of 0.25 Å and close to the barrier in steps of 0.125 Å) decrease $L_{\mathrm{Al-O_2}}$, always using the converged orbitals of one step as starting guess for the next calculation. This "creeping" procedure works very well most of the time, ensuring rapid convergence. However, the abrupt spin changes encountered as charge transfer is initiated will sometimes cause the algorithm to stick to one diabatic energy surface too long. Since further decrease of $L_{\mathrm{Al-O_2}}$ (or increase of $L_{\mathrm{O-O}}$) will ultimately find the correct spin configuration where charge transfer already occurred, the true adiabatic potential energy surface is easily recovered by in turn creeping towards larger $L_{\mathrm{Al-O_2}}$ (and respectively smaller $L_{\mathrm{O-O}}$) to map out the second diabatic potential energy surface, until the crossing point of the different diabatic surfaces is found.

ERROR ESTIMATES

To assess the accuracy of our approach, we perform further calculations for the bridge site and O_2 parallel incidence, as well as for the fcc hollow site and O_2 perpendicular incidence (i.e., the two potential energy surfaces discussed in the main manuscript). We calculate a part of the PES going from reactants to past the saddle point, $L_{\mathrm{O-O}} \in [1.2, 1.4]$ Å and $L_{\mathrm{Al-O_2}} \in [1.5, 5]$ Å. We consider different cluster geometries and different basis sets. In the case of "perfect" embedding, our results should not depend on the geometry choice. Since we do not allow for exchange of charge between cluster and environment, the cluster must not be too small, otherwise the charging energy of the cluster distorts the barrier height. Atoms in the second layer are essential to correctly describe screening effects. A reliable estimate for the barrier requires clusters containing at least 10 Al atoms (see data for bridge cluster, Tab. 1), while smaller clusters overestimate the energy cost to initiate charge transfer, and hence the barrier. Fluctuations in barrier height for different cluster geometries are $\lesssim 60$ meV.

We observe a very weak dependence of barrier height on basis set choice. The SBKJC basis set and effective core potential are a well-established, accurate way to treat only electrons of the outer shell for lighter elements like aluminum and oxygen[12]. The associated computational cost unfortunately precludes using SBKJC for the entire cluster. To verify that this does not lead to large errors, we compare barrier heights for the same cluster geometry but different basis sets and effective core potentials. Calculations yield a change in barrier below 6 meV (LANL2DZ on all atoms vs. the full basis set that uses SBKJC and LANL2DZ as described earlier; see fcc site, Tab. 1). The reason for this is a favorable cancellation of systematic basis set errors in the subtraction of Eq. 1 coupled with the still considerable distance between O and the Al(111) surface at the barrier (> 2 Å).

The importance of including the embedding potential is made clear by comparing to calculations on bare clusters, and to calculations corrected by Eq. 1 with $V_{\mathrm{emb}} \equiv 0$, equivalent to the ONIOM method of Morokuma and coworkers [14]. Non-embedded cluster models yield potential energy surfaces containing barriers, but the quantitative and relative barrier height is not reliable (see Tab. 1, specifically the fcc result). In particular, the relative barrier heights for the two different adsorption sites are reversed from those implied by experiment, leading to qualitatively wrong predictions for the dominant adsorption path.

The accuracy of the CASPT2 method is well established for the atoms at hand [15, 16]. To estimate the entropy contribution (due to vibrational excitations of the O_2 molecule) to the barriers, each saddle point is fitted with a parabola to estimate the zero-point vibrational energy using free O_2 at $L_{\mathrm{Al-O_2}} = 5$ Å as a reference. The entropic corrections are found to be less than 30 meV. We find fluctuations in the potential energy surface (for adjacent points) below 30 meV (see Tab. 1 here and in the main manuscript).

Concerning convergence with cluster size, we find minor changes upon reaching clusters of more than 12 atoms (see Fig. 1). Smaller clusters tend to overestimate barrier heights. This error is further compounded by the non-self consistent embedding. To estimate an upper bound of a resulting error, we consider the energy difference $\Delta\varepsilon$ between the ionization energy of an Al atom (≈ 6 eV) and the work function of an Al surface (≈ 4 eV), $\Delta\varepsilon \approx 2$ eV. As clusters become larger, we expect the ionization

energy of the cluster to approach the Al surface limit at least as

$$E_{\rm ion}^{\rm cluster} = E_{\rm ion}^{\rm surface} \pm \Delta\varepsilon/N, \qquad (2)$$

where N is the number of cluster atoms. Fluctuations in barrier height stay well within this estimate (see error bars in Fig. 1). In summary, we thus estimate 100 meV as an upper bound for the uncertainty of our barrier heights.

Considering even larger clusters (i.e., to extend Fig. 1 to the right) is computationally prohibitive for two reasons: not only does the correlated wavefunction method scale badly with the number of atoms but clusters with more atoms also feature smaller energy level spacings. Consequently, a larger number of cluster orbitals with energies close to the Fermi level need to be included in the CAS for larger clusters to account for these near-degeneracies. Since the CASSCF calculation scales factorially with CAS size, we are not able to extend the CAS size sufficiently to achieve smooth PESs (one indicator of a converged CAS size) for clusters larger than 14 atoms. Note that this is not related to an underlying failure or divergence of the CASSCF/CASPT2 approach, but simply to a prohibitively large computational cost.

Finally, we note that the embedded cluster calculation only yields a correction to the DFT PESs. Effects like the interaction of the approaching molecule with its image charge, which would not be well represented solely based on a cluster calculation, are already included in the DFT calculation. Indeed, the correlated wavefunction calculations mainly need to correct [see Eq. (1)] for short-ranged correlation effects, which are well accounted for by the cluster size considered here.

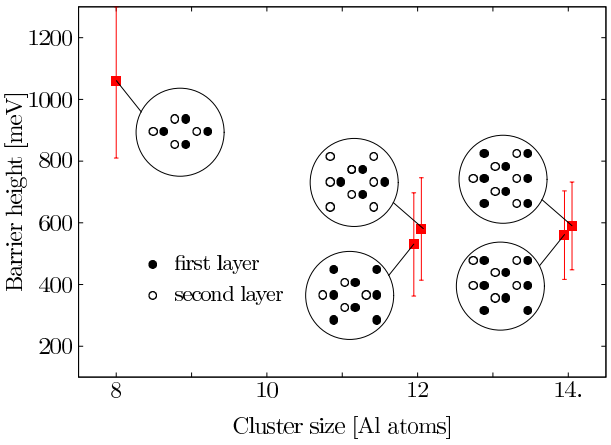

FIG. 1. (Color online) Convergence of the barrier height with respect to embedded cluster size for the bridge site and O_2 parallel incidence (compare numbers in Tab. 1). Data points at identical cluster sizes are slightly displaced for visual clarity. Error bars estimate the error due to a fixed charge on the cluster [see Eq. (2)].

As a further consistency check, we investigate the energetics for the adsorbed oxygen molecule. We calculate the energy $E_{\rm O}$ of a single oxygen atom close to the Al (111) surface. We find two minima (at the fcc and hcp positions), with a respective energy gain (with respect to a O-surface distance of 5 Å) of 8.3 and 8.1 eV. By contrast, the corresponding embedded potential energy surface (E-PES) for the oxygen molecule features a minimum of $E_{\rm emb} = -6.8$ eV (relative to the energy at 5 Å distance) at $L_{\rm O-O} = 2.2$ Å and $L_{\rm Al-O_2} = 0.9$ Å [see Fig. 2(c) in the main manuscript]. The larger value of $L_{\rm O-O} = 2.2$ Å for the adsorbed molecule as compared to the distance between the hcp and fcc surface positions (1.66 Å) is due to Coulomb repulsion between the two charged oxygen atoms. Modifying $E_{\rm O}$ by the Coulomb repulsion due to the presence of a second O (both negatively charged due to charge transfer) at an adjacent hcp site yields a shifted minimum at a bond length of $L_{\rm O-O} = 2.3$ Å, in good agreement with the E-PES. The electrostatic repulsion energy [taking a Mulliken charge of ≈ 0.75e from Fig. 3(e) in the main text] is 3.7 eV, and the bond dissociation energy of $O_2 \approx 4.9$ eV (using CASPT2). Hence, a rough estimate predicts $8.3 + 8.1 - 4.9 - 3.7 = 7.8$ eV dissociative adsorption energy for the O_2 molecule. Considering the simplicity of this argument, the agreement with the minimum of our potential energy surface (6.8 eV) is satisfying.

# atoms $1^{\rm st}/2^{\rm nd}$ layer	$E^{\rm Barrier} \pm \delta$ [meV]	$L^{\rm Barrier}_{\rm Al-O_2}$ [Å]	Notes
bridge, parallel orientation			
4/4	1060 ± 10	2.4	only 8 atoms
8/4	530 ± 10	2.3	
4/8	580 ± 15	2.2	
8/6	590 ± 10	2.4	
8/6	560 ± 20	2.4	alternative geometry
8/6	620 ± 15	2.2	bare
8/6	500 ± 15	2.2	Eq. 1, $V_{\rm emb} \equiv 0$
fcc, perpendicular orientation			
6/6	363 ± 10	2.9	Full basis set
6/6	357 ± 20	2.4	LANL2DZ basis set
6/6	1200 ± 15	2.5	bare
6/6	980 ± 10	2.4	Eq. 1, $V_{\rm emb} \equiv 0$

TABLE I. Embedded-CW predictions of the barrier height and surface distance at the top of the barrier for different cluster sizes and cluster geometries (bridge site, see also Fig. 1), as well as different basis sets (fcc site). Results for bare clusters (i.e., non-embedded calculations), and for using Eq. (1) with $V_{\rm emb} \equiv 0$ are provided as well. Errors represent fluctuations in the final embedded potential energy surface.

* eac@princeton.edu

[1] G. Kresse and J. Furthmüller, Computational Materials Science **6**, 15 (1996).
[2] J. P. Perdew, K. Burke, and M. Ernzerhof, Physical Review Letters **77**, 3865 (1996).
[3] G. Laramore and C. Duke, Physical Review B **5**, 267

(1972).
[4] M. A. van Hove, W. H. Weinberg, and C.-M. Chan, *Low-Energy Electron Diffraction*, Surface Sciences (Springer Verlag, Berlin, 1986).
[5] C. Huang, M. Pavone, and E. A. Carter, J Chem Phys **134**, 154110 (2011).
[6] X. Gonze, B. Amadon, P.-M. Anglade, J.-M. Beuken, F. Bottin, P. Boulanger, F. B. and' D. Caliste, R. Caracas, M. Cote, T. Deutsch, L. Genovese, P. Ghosez, M. Giantomassi, S. Goedecker, D. Hamann, P. Hermet, F. Jollet, G. Jomard, S. Leroux, M. Mancini, S. Mazevet, M. Oliveira, G. Onida, Y. Pouillon, T. Rangel, G.-M. Rignanese, D. Sangalli, R. Shaltaf, M. Torrent, M. Verstraete, G. Zerah, and J. Zwanziger, Computer Phys. Commun. **180**, 2582 (2009).
[7] X. Gonze, G.-M. Rignanese, M. Verstraete, J.-M. Beuken, Y. Pouillon, R. Caracas, F. Jollet, M. Torrent, G. Zerah, M. Mikami, P. Ghosez, M. Veithen, J.-Y. Raty, V. Olevano, F. Bruneval, L. Reining, R. Godby, G. Onida, D. Hamann, and D. Allan, Zeit. Kristallogr. **220**, 558 (2005).
[8] N. Troullier and J.-L. Martins, Physical Review B **43**, 1993 (1991).
[9] F. Aquilante, L. De Vico, N. Ferré, G. Ghigo, P.-A. Malmqvist, P. Neogrády, T. B. Pedersen, M. Pitonák, M. Reiher, B. O. Roos, L. Serrano-Andrés, M. Urban, V. Veryazov, and R. Lindh, J Comput Chem **31**, 224 (2010).
[10] M. W. Schmidt, K. K. Baldridge, J. A. Boatz, S. T. Elbert, M. S. Gordon, J. H. Jensen, S. Koseki, N. Matsunaga, A. Nguyen, S. Su, T. L. Windus, M. Dupuis, and J. A. Montgomery, Comput. Chem. **14**, 1347 (1993).
[11] M. S. Gordon, "Theory and applications of computational chemistry: the first forty years," (Elsevier, Amsterdam, 2005) Chap. Advances in electronic structure theory: GAMESS a decade later, p. 1167.
[12] W. J. Stevens, H. Basch, and M. Krauss, The Journal of Chemical Physics **81**, 6026 (1984).
[13] P. J. Hay and W. R. Wadt, The Journal of Chemical Physics **82**, 270 (1985).
[14] M. Svensson, S. Humbel, R. D. J. Froese, T. Matsubara, S. Sieber, and K. Morokuma, Journal of Physical Chemistry **100**, 19357 (1996).
[15] K. Andersson, P.-A. Malmqvist, and B. O. Roos, The Journal of Chemical Physics **96**, 1218 (Sep 1992).
[16] N. Forsberg and P.-Ă. Malmqvist, Chemical Physics Letters **274**, 196 (1997).